

2019

A new oncogenic function of the glycolytic enzyme lactate dehydrogenase-A in small cell lung cancer

<https://hdl.handle.net/2144/36338>

"Downloaded from OpenBU. Boston University's institutional repository."

BOSTON UNIVERSITY
SCHOOL OF MEDICINE

Thesis

**A NEW ONCOGENIC FUNCTION OF THE GLYCOLYTIC ENZYME
LACTATE DEHYDROGENASE-A IN SMALL CELL LUNG CANCER**

by

TOBIN GRAMYK

B.A., University of San Diego, 2016

Submitted in partial fulfillment of the
requirements for the degree of
Master of Science

2019

© 2019 by
TOBIN GRAMYK
All rights reserved

Approved by

First Reader

Vickery Trinkaus-Randall, Ph.D.
Professor, Biochemistry

Second Reader

Yujiang Geno Shi, Ph.D.
Associate Biochemist, Brigham and Women's Hospital, Associate
Professor of Medicine, Harvard Medical School

ACKNOWLEDGMENTS

I would like to thank Yujiang Geno Shi, Ph.D, who served as my PI over the course of my research. Additionally, Yujuan Jin was a tremendous help and guided me throughout the course of the project and provided thoughtful and necessary discussions and assisted with many of the experiments I completed. I would also like to thank my first reader, Vickery Trinkaus-Randall, Ph.D., who has also assisted in mentoring me.

**A NEW ONCOGENIC FUNCTION OF THE GLYCOLYTIC ENZYME
LACTATE DEHYDROGENASE-A IN SMALL CELL LUNG CANCER**

TOBIN GRAMYK

ABSTRACT

Small Cell Lung Cancer (SCLC) is an epithelial cancer that has, until recent years, been labeled a recalcitrant tumor type. Since its discovery and classification, there has been very little research to understand and treat SCLC. Conventional methods of treatment for SCLC include chemotherapeutics have been used with little long-term success. Following initial treatment, the cancer appears to be fully wiped out, however seemingly without fail the cancer reemerges with acquired drug resistance and the capability to rapidly metastasize, leading to a five-year survival rate of less than 10%. While there have been continuous improvements in the field of cancer therapeutics, combining chemotherapeutics and immunotherapy, there has been no targeted clinical therapy for SCLC. Recent studies have suggested that an acidic tumor microenvironment is highly important for the progression of other cancers. LDHA generates lactate from pyruvate, leading to a more acidic environment, which indicates LDHA may be a viable target for cancer therapeutics. CRISPR-cas9 gene editing and mouse SCLC cell lines were used to study lactate concentration and cell vitality. After analysis of several different SCLC tumors, larger tumors had both a higher metastatic capability and higher concentrations of lactate, indicating that LDHA was more highly active in these tumors. CRISPR-cas9 knockout targeting of LDHA decreased SCLC colony formation and

cellular growth *in vitro*, leading to the conclusion that LDHA may play a vital role in the future as a potential therapeutic target for the treatment of SCLC.

TABLE OF CONTENTS

| | |
|----------------------------|------|
| TITLE..... | i |
| COPYRIGHT PAGE..... | ii |
| READER APPROVAL PAGE..... | iii |
| ACKNOWLEDGMENTS | iv |
| ABSTRACT..... | v |
| TABLE OF CONTENTS..... | vii |
| LIST OF TABLES | viii |
| LIST OF FIGURES | ix |
| LIST OF ABBREVIATIONS..... | xi |
| INTRODUCTION | 1 |
| SPECIFIC AIMS | 15 |
| METHODS | 16 |
| RESULTS | 24 |
| DISCUSSION | 37 |
| REFERENCES | 42 |
| VITA..... | 49 |

LIST OF TABLES

| Table | Title | Page |
|-------|---|------|
| 1 | List of Primers used for enzyme cutting in plasmid design | 17 |
| 2 | Concentration of pCDH Plasmids before ligation | 23 |
| 3 | Protein Concentration of MCF-7 hLDHA sgRNA cells | 24 |

LIST OF FIGURES

| Figure | Title | Page |
|--------|---|------|
| 1 | Schematic Diagram of Glycolysis | 5 |
| 2 | HIF1a and LDHA Interaction | 7 |
| 3 | Protein Detection of hLDHA sgRNA in MCF-7 Cells | 24 |
| 4 | Western Blot of 2-day Puromycin Selection MCF-7 Cells | 25 |
| 5 | Western Blot of hLDHA-KO in MCF-7 and A549 Cells | 26 |
| 6 | IF Staining of A549 WT Cells in Full Medium | 26 |
| 7 | IF Staining of A549 WT Cells with Lactate Treatment | 27 |
| 8 | IF Staining of A549 CRISPR V2 Cells in Full Medium | 27 |
| 9 | IF Staining of A549 CRISPR V2 Cells Lactate Treatment | 28 |
| 10 | IF Staining of A549 hLDHA sg1 in Full Medium | 28 |
| 11 | Translocation of LDHA into the Nucleus | 29 |
| 12 | Concentration of Lactate in Different Sized Tumors | 30 |
| 13 | Expression of LDHA in 716T2S Cell Line | 31 |
| 14 | Lactate Concentration in Mouse SCLC Cells | 31 |
| 15 | Western Blot of LDHA-KO in Mouse SCLC Cells | 32 |
| 16 | Lactate Concentration in 716T2S-LDHA-KO Cells | 32 |
| 17 | Colony Formation of 716T2S-LDHA-KO cells | 33 |
| 18 | Colony Counting of 716T2S-LDHA-KO Cells | 33 |

| | | |
|----|---|----|
| 19 | Cellular Growth of 716T2S-LDHA-KO Cells | 34 |
| 20 | Western Blot of 728N-LDHA-KO Cells | 34 |
| 21 | Colony Formation of 728N-LDHA-KO Cells | 35 |
| 22 | Colony Counting of 728N-LDHA-KO Cells | 35 |
| 23 | Cellular Growth of 728N-LDHA-KO Cells | 36 |

LIST OF ABBREVIATIONS

| | |
|-------------|---|
| BU..... | Boston University |
| CRISPR..... | Clustered Regularly Interspaced Short Palindromic Repeats |
| dNTP..... | Deoxyribonucleotide Triphosphate |
| HRP..... | Horseradish Peroxidase |
| KO..... | Knock Out |
| LDHA..... | Lactate Dehydrogenase A |
| PCR..... | Polymerase Chain Reaction |
| SCLC..... | Small Cell Lung Carcinoma (Cancer) |
| WT..... | Wild Type |

INTRODUCTION

Cancer is the cause of about twenty-five percent of deaths in the United States. Frustratingly, there is a rise in the number of incidences of cancer, mainly due to an increased population size, a higher life expectancy, and various other risk factors such as smoking, decreased activity, and a rise in obesity. Globally, breast cancer is diagnosed the most frequently in females and similarly it is the cancer that has the highest death rate among females. In Northern America, there is an elevated incidence of breast cancer, and currently there are no direct cures for this cancer (Torre et al., 2015). Cancer is marked by several factors found throughout its development. There is a contemporary list of six hallmarks of cancer that include: Ongoing proliferative signaling, evasion of growth suppressors, resistance to cell death, unending replication, the induction of angiogenesis, and the ability to invade and metastasize to different tissues. Furthermore, these hallmarks are found with genomic instability which provides fertile ground for continued mutations that generate genetic diversity which in turn support the hallmarks of cancer. Recently, two new functions have become entwined in cancer; the distorted energy metabolism found in cancers as well as the ability to avoid destruction by the immune system. Additionally, it has been discovered that the microenvironment surrounding the tumor differs from the normal environment, still utilizing seemingly normal cells to create a healthier environment for the tumor (Hanahan & Weinberg, 2011). More specifically, a creation of metabolism specific hallmarks of cancer has been established. Among these metabolic hallmarks are: the dysregulated uptake of glucose and amino acids, utilization of wolfish methods to acquire nutrients, taking advantage of metabolic

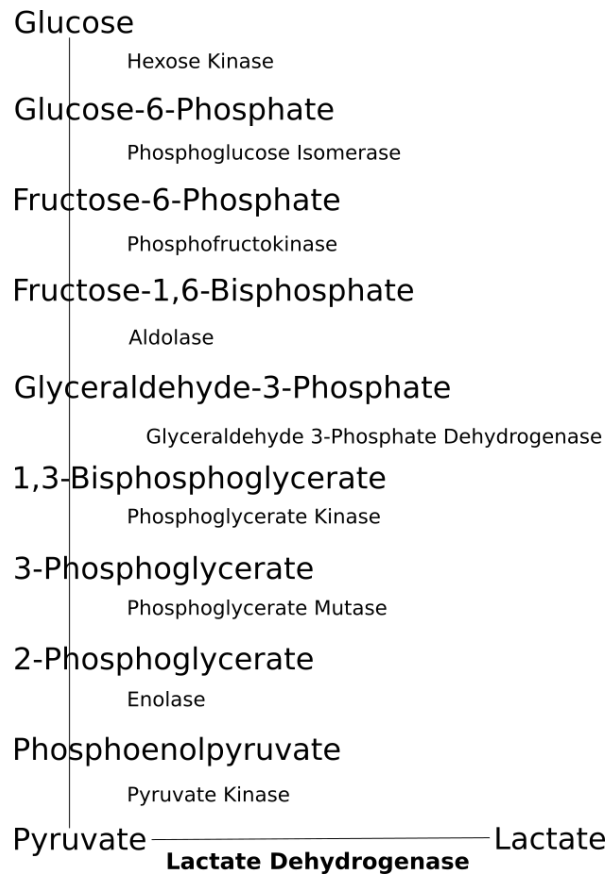
intermediates for biosynthesis and generation of NADPH, a higher need for nitrogen, changes in gene regulation driven by metabolites, and the specific interactions between the microenvironment and the metabolites. Identification and further classification of these hallmarks is a point of continued research in the cancer field. The hope is that additional knowledge will elucidate novel targets for targeted therapy and the eventual cure to cancer (Pavlova & Thompson, 2016).

Glycolysis is an important source of ATP in many organisms. While it is not as efficient as aerobic respiration in terms of generating ATP, it has been found to play an important role in cancers. The enzymes involved in the biochemical pathway of glycolysis have been shown to have secondary functions that were previously unknown. LDHA, previously known to oxidize NADH to NAD⁺ through reduction of pyruvate to lactate has now been shown to have a role in transcriptional regulation of Histone 2B. This secondary role opens the door to examine the interaction between a glycolytic enzyme, such as LDHA, and its potential role in cancer (Kim & Dang, 2005). Under normal conditions, LDH is expressed in both skeletal and cardiac muscle. It is comprised of two separate isoenzymes in a tetrameric arrangement. The two subunits are M and H. In total, there are five different combinations that have been completely characterized, that vary in the amount of each subunit present. Each isoform of LDH is a tetramer, that differs in the composition of subunits; in total there are five classified isoforms (Markert, 1963) (Seth et al., 2011). LDHA is comprised of four M subunits and is the form most commonly found in skeletal muscles. LDHB consists of four H subunits and is found in the heart. LDHA and LDHB have different characteristics and function differently.

LDHA is not inhibited by high concentrations of pyruvate whereas LDHB is inhibited by high concentrations of pyruvate. This difference indicates that LDHA is the isoform that preferentially produces lactate while LDHB preferentially produces pyruvate (Gray, Tompkins, & Taylor, 2014). An interesting phenomenon found in cancer cells is the use of glycolysis in the presence of ample oxygen. This was first identified by Otto Warburg and labeled “The Warburg Effect” or Aerobic Glycolysis (Liberti & Locasale, 2016) (Ždralević et al., 2018). Normal cells will primarily use oxidative phosphorylation as the main source of ATP generation as it is vastly more efficient and has a higher capacity for creation. The purpose of this aerobic glycolysis is still debated, but a compelling argument for its function has recently emerged. It is proposed that aerobic glycolysis is utilized by cancer cells, as well as other proliferating cells, to promote the uptake and subsequent incorporation of the required nutrients for growth into the cell biomass (Parra-Bonilla, Alvarez, Al-Mehdi, Alexeyev, & Stevens, 2010). The reasoning supporting this idea is found in the activation of signaling pathways for cell proliferation also plays a role in regulating the metabolic pathways that control nutrient uptake, as well as specific mutations found in cancer cells that give them the ability to better proliferate rather than have efficient ATP generation. The proliferation of a normal cell is controlled by the presence of growth factors, as without these growth factors, normal cells cannot proliferate uncontrollably. It is found that cancer cells develop a genetic mutation that changes the growth factor signaling pathway in such a way that the cell will continuously uptake nutrients required for cell growth. The most important factor that is taken into the cell and metabolized is, of course, glucose (Vander Heiden, Cantley, & Thompson,

2009). The mechanism of this uptake is found in the upregulation in several key components of the glycolytic pathway. First, to get the glucose into the cell, there is an upregulation in the glucose transports GLUT 1 and GLUT 3. Second, an important enzyme isoform, Hexokinase II will interact with the mitochondria via a voltage-dependent anionic channel. Third, Phosphofructokinase becomes overactive as it's L and P isoforms predominate and the overexpression of PFKB3 causes higher levels of fructose-2,6-biphosphate which serve to further enhance the activity of PFK. Fourth, another isoform of Pyruvate kinase, M2, is responsible for regulation of the glycolytic flux and enhances metabolite accumulation within the cell to meet its growth needs. Importantly, the M-isoform of LDH is overexpressed, which will lead to a build-up of lactate and more acidic pH. Lastly, other mutations in the glycolytic pathway will disrupt transport of metabolites into the mitochondria as well as decrease the ability of the mitochondrial respiratory complexes to generate ATP (Fadaka et al., 2017).

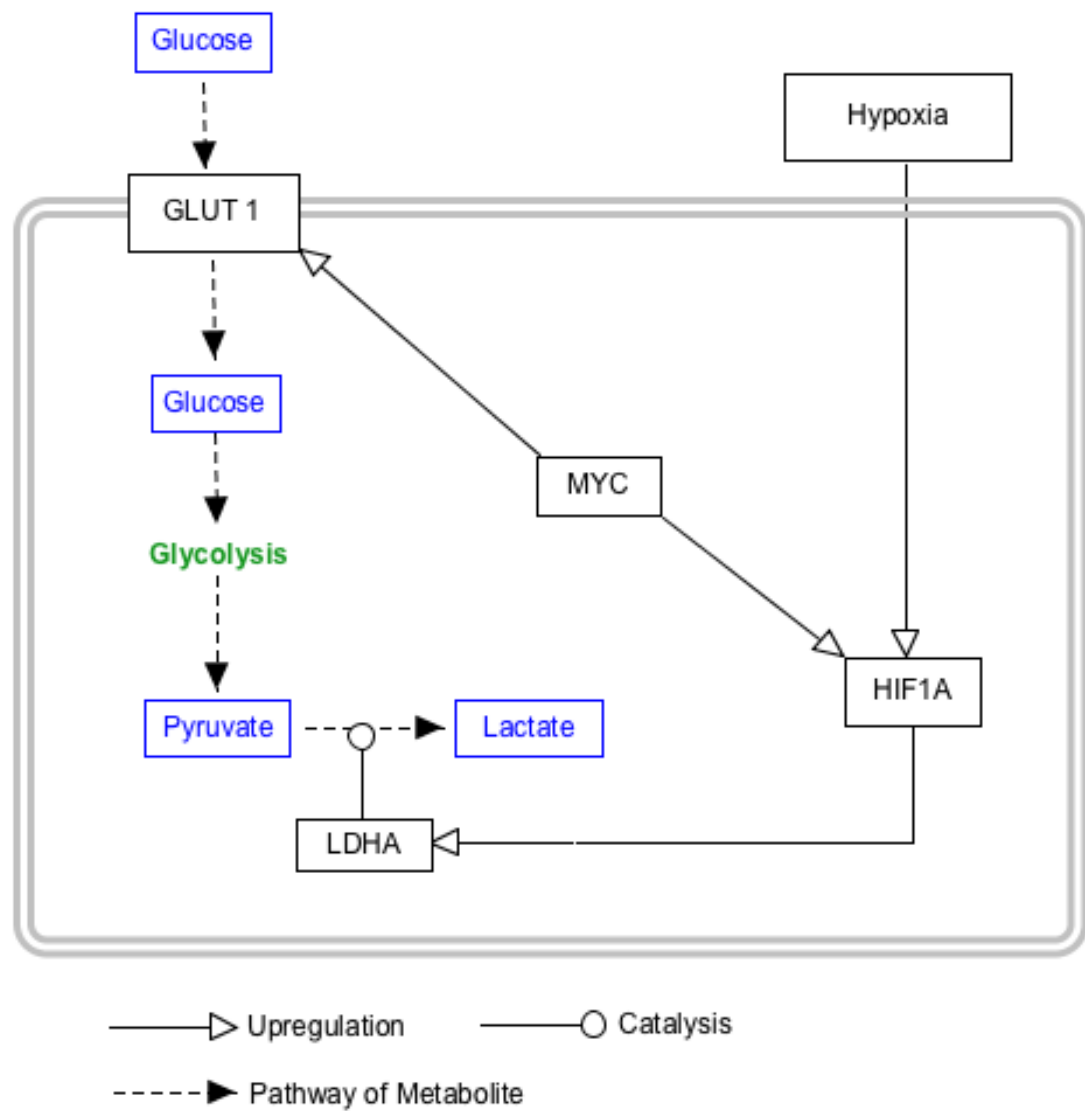
Figure 1: **Schematic diagram of Glycolysis**. In bold is the enzyme of importance in this study, LDH. LDH catalyzes the conversion of the reversible reaction of Pyruvate, the final result of glycolysis, into Lactate.



Hypoxia is a common element found in cancer cells. This is due to the rapid growth of the cancer cells as they outgrow the capacity of their vascular supply, which thereby limits the amount of oxygen that is able to diffuse into the tumor. Cancer cells have developed methods to combat this, and often times cancers show increased expression of Hypoxia Induced Factor 1 α (HIF1 α) (Masoud & Li, 2015) (Rhim, Lee, & Lee, 2013). Interestingly, this expression is also increased in a hypoxia-independent mechanism, done by the master regulator MYC. Both hypoxic conditions and the oncogenic activity of the MYC increase the LDHA expression in cells. Additionally, activation of MYC causes an increase in the expression of a GLUT1 transporter that is

responsible for the uptake of glucose into the cell (Osthus et al., 2000). MYC has been implicated in other studies as having the ability to upregulate other glycolytic enzymes such as Hexokinase II, Phosphofructokinase, and Enolase 1. The upregulation of these enzymes contributes to the Warburg effect and has been postulated to increase the cellular invasion capability of cancer cells. Interestingly, it was found that MYC upregulation produced lactic acid and only LDHA upregulation produced increased levels of lactate, pointing to LDHA as a promotor of the Warburg effect. (Miller, Thomas, Islam, Muench, & Sedoris, 2012). This points to one hallmark of cancer, which is the changed metabolism (Majmundar, Wong, & Simon, 2010).

Figure 2: **HIF1A and LDHA Interaction.** HIF1A is upregulated by hypoxic conditions in the cell as well as by MYC in a non-hypoxia dependent manner. Activation of HIF1A causes an increase in the expression of LDHA, which favors the production of Lactate and creates an increasingly acidic microenvironment around the cell.



Tumor hypoxia has also been found to stimulate an epithelial-to-mesenchymal transition (EMT), which increases the metastatic capacity of the tumor as well as cellular mobility. It has also been posited that this transition also provides the cancer cells with increased drug resistance through its ability to stimulate cell quiescence (Muz, de la Puente, Azab, & Azab, 2015). LDH has been shown to be involved with the OCA-S

complex, which is a co-activation complex which is important in the activation of the Histone H2B Promoter. The importance of this relation between the two is found in the OCA-S complex's location inside of the nucleus. This finding provides evidence that LDH could also be found within the nucleus, and perhaps could link the OCA-S complex to the redox state of the cell. Thus, it is important to determine how disruptions to LDH can impact the transcription of certain factors in the cell (Zheng, Roeder, & Luo, 2003).

Interestingly, the translocation of LDHA into the nucleus has been reported all the way back into last century. However, the purpose and the mechanism of this translocation has yet to be elucidated. One study identified a nucleic acid helix-destabilizing protein as Lactate Dehydrogenase-5, commonly known as Lactate Dehydrogenase A (Williams, Reddigari, & Patel, 1985). This finding shows the possibility of biological proteins having multiple roles that may depend on the current location of the protein. Another related study showed again that a low-salt-eluting single stranded DNA (ssDNA) binding protein derived from a mouse myeloma is identical to a mouse LDHA subunit. This was determined through analysis of identical apparent molecular masses and the cross-reactions between both mouse and bovine LDHA subunits (Sharief, Wilson, & Li, 1986). Furthermore, it has been found that Lactate Dehydrogenase functions as a single-stranded DNA binding protein that specifically affects the DNA-polymerase-alpha primase complex. This was proven via testing the binding preference of the LDH to ssDNA to double stranded DNA (dsDNA) and LDH was shown to have a 300 fold affinity for binding the ssDNA (Grosse, Nasheuer, Scholtissek, & Schomburg, 1986).

It has been found that LDHA functions outside of its glycolytic role (Seki & Gaultier, 2017). Specifically, it has been found to increase the invasion potential of cancer cells, provide resistance to anoikis, as well as increase the metastatic capability of the tumor. It has been postulated that the phosphorylation of specific residues on LDHA cause increased activity and the negative effects. Specifically, it was found that phosphorylation of Tyrosine 10 (Y10) was completed by two kinases, HER2 and Src. This phosphorylation and therefore increased LDHA activity was found to correlate with breast cancer tumors that were metastatic. Importantly, it was shown that inhibition of these two kinases decreased LDHA activity and limited the invasion capability, anoikis resistance, and metastatic potential (Jin et al., 2017).

Because of LDHA's important role converting pyruvate to lactate, it has earned the distinction of being a checkpoint of anaerobic glycolysis. It is also found to be elevated in many different cancer types, thereby implicating it as a potential diagnostic or therapeutic target for the inhibition of cancer (Miao, Sheng, Sun, Liu, & Huang, 2013). Some studies have found success in reducing tumor growth *in vitro* through the inhibition of a glucose transporter and LDHA (Ooi & Gomperts, 2015) In pancreatic cancers, it was found that acetylation status determined the activity of LDHA. This is in contrast to phosphorylation playing an important role in the activation of LDHA in other forms of cancer. Normally, LDHA is acetylated and therefore inhibited, however pancreatic cancers have a reduced amount of acetylation of LDHA and subsequently increased protein levels of LDHA. A genetic study investigating Tamoxifen-resistant breast carcinomas used genetic clustering to determine the gene expression of these carcinomas.

What was found was that LDHA was upregulated in these conditions, pointing to LDHA's potential importance in drug resistance (Jansen et al., 2005). Interestingly, LDHA's role in the progression of pituitary adenomas has also been studied. In this cancer type, it was found that the highly invasive pituitary adenomas exhibited significantly raised levels of both LDHA mRNA and protein expression. This study also utilized the LDHA inhibitor Oxamate to successfully decrease the invasive and proliferative ability of primary pituitary adenoma cell cultures. This demonstrated the use of Oxamate in an *in vivo* situation to inhibit LDHA, demonstrating its potential viability (An et al., 2017).

Significantly, LDHA has been implicated in the tumor's ability to evade the immune system and supply the tumor with resistance to chemotherapeutic agents. A recent study showed that LDHA granted the tumor the ability to evade the immune system. Through looking at the effects of LDHA expressed by macrophages in a murine lung carcinoma model, it was determined that LDHA and lactate expressions by the macrophages drove T-cell immunosuppression. It was found that specific deletion of LDHA in the myeloid cells promoted a tumor suppressive phenotype of macrophages (Seth et al., 2017). This study confirmed the viability of targeting LDHA in combination with other drugs as a productive treatment for cancer therapy. Drug resistance is a major concern when dealing with cancer cells. Studies have demonstrated that LDHA in combination with HIF1A in multiple myeloma cells contributes to drug resistance. Furthermore, this study showed through the inhibition of LDHA and HIF1A that sensitivity of the cancer cells to therapeutic agents was restored. Additionally, knock

down of LDHA restored sensitivity to the therapeutic agent in drug resistant tumor cells, while gain of function studies using LDHA and HIF1A caused drug resistance in cell lines previously sensitive to therapeutic agents (Maiso et al., 2015). Similarly, another study looking at ErbB2-positive breast cancer found that increased glycolysis through heat shock factor 1 and LDHA contributed to resistance to a therapeutic agent (Zhao et al., 2009). Furthermore, it was shown that specific inhibition of glycolysis and therefore LDHA increased the therapeutic efficacy of the therapeutic agent in the treatment of ErbB2-positive breast cancers. It was found that ErbB2 upregulated both LDHA and heat shock factor 1. It was through ErbB2 dependent upregulation of heat shock factor 1 that caused heat shock factor 1 to bind to the LDHA promotor and therefore increase LDHA expression. Furthermore, inhibition of glycolysis and of LDHA specifically through Oxamate showed selectively inhibited growth of the ErbB2 cells (Zhao et al., 2009). These results showed the impact that LDHA has on the invasive potential of the cancer cell and the potential to decrease that potential. Another study showed the high glycolytic activity of melanomas resulted in an increased acidification of the tumor microenvironment. This acidification had the effect of activating a GPCR-dependent expression of ICER, which is a transcriptional repressor, in tumor-associated macrophages. This expression caused a shift in the functional polarization of the macrophages into a non-inflammatory phenotype, which not only contributed to tumor growth, but also assisted with immunoevasion (Bohn et al., 2018). This increased acidification was found to have mostly come from the build-up of lactic acid production, caused by LDHA. Importantly, another study found that by using bicarbonate to

neutralize the acidic microenvironment around the tumor, there was improvement in the effectiveness of immunotherapy for some solid tumors (Pilon-Thomas et al., 2016). This is useful because if this treatment has already been shown effective, then blockage of tumor acidity on the upstream side might prove to be an effective treatment strategy. Other studies have sought to identify compounds that exert inhibitory effects against LDHA, even identifying a compound with an IC_{50} of 0.36 μ M (Li, Xiao, & Zhao, 2017).

Small Cell Lung Cancer (SCLC), is an epithelial cancer that comprises about 15% of all lung cancers, but it displays unique features that distinguish it from non-small cell lung cancer (NSCLC). Notably, SCLC is typically a neuroendocrine tumor, while still maintaining some important heterogeneity in cell type. There are several important neuroendocrine markers found in SCLC most importantly including: Achaete-scute homologue 1 (ASCL1) which is a transcription factor and ASCL1, which is responsible for induction of neuronal and neuroendocrine differentiation. Importantly, neurogenic differentiation factor 1 (NEUROD1), is a master regulator of neuronal expression that works in combination with ASCL1. Interestingly, NEUROD1 targets the oncogene MYC, which in turn is able to activate LDHA as LDHA is a MYC responsive gene (Zeller, Jegga, Aronow, O'Donnell, & Dang, 2003). Recently, it has been found that Re1 silencing transcription factor (REST) has an important role in SCLC by repressing the expression of the neuroendocrine differentiation of cells. SCLC presents with swift tumor growth, high vascularity, and introduces instability into the genome. Additionally, in almost every single SCLC, there is inactivation of the tumor suppressors TP53 and RB1, which seem to be the most important factors in preventing the SCLC phenotype

from developing. Unfortunately, SCLC is also a highly metastatic cancer type and while SCLC often responds well initially to chemotherapy, seemingly without fail, it typically relapses quickly while obtaining resistance to further chemotherapeutic treatment (Y. Chen, Yang, Xu, Cao, & Chen, 2017). Until recently, there have been very few notable developments in treatment practices for SCLC as the standard of care has been doublet chemotherapy using a platinum agent and etoposide (Rudin et al., 2015). Another notable difficulty of dealing with SCLC both clinically and approaching it from the research side is the lack of available tumor samples. SCLC is a highly metastatic cancer type and its discovery can often be at a secondary site. This, along with the fact that the tumor composition can vary in the amount of neuroendocrine and non-neuroendocrine cells present make using cell lines difficult as they are not always faithful recreations (Gazdar, Bunn, & Minna, 2017). While there is not much use of Induced Pluripotent Stem Cells (iPSCs), one study reported ASXL3, a PRC2-associated protein, as a novel epigenetic target for treatment of SCLC (Shukla et al., 2017).

In lung cancers, LDH has been used as a prognostic marker for the prognosis of the disease. Data from one study suggested that patients that had a higher level of serum LDH prior to treatment were more likely to have worse overall survival percentages (Deng, Zhang, Meng, Zhou, & Li, 2018). Similarly, another study sought to validate LDH as a marker to monitor treatment response in SCLC. The results from this study showed that elevated levels of LDH corresponded with a higher likelihood of disease progression and that again, high initial levels of LDH correlated with a decreased probability of patient survival (C. Chen, Zhu, & Huang, 2018). Intriguingly, another

method for measuring survival in lung cancer patients is to look at circulating tumor cell count (CTC). LDH has been previously thought to be involved with the metastatic capabilities of cancers. One study determined that higher amounts of CTCs caused decreased progression free survival and overall survival. It is highly likely that LDH plays a role in this process, and the correlation between increased CTC and decreased survivability indicate that targeting LDH in SCLC may be a potential successful therapeutic avenue.

SPECIFIC AIMS

The purpose of this thesis is to investigate the role of Lactate Dehydrogenase A (LDHA) in the promotion of Small Cell Lung Cancer (SCLC). SCLC is a highly metastatic cancer that easily spreads to the brain. It is not known what causes the highly invasive nature of this cancer type. LDHA has been thought to play a role in the ability of the tumor to metastasize. In this study we hope to determine whether there is a similar role of LDHA in SCLC and if the removal of LDHA from the cell line attenuates the metastatic capacity of the tumor. Additionally, based on previous literature and our observations, we sought to determine what factors stimulated the translocation of LDHA from the cytoplasm into the nucleus.

METHODS

Image Generation

Pathway images were generated using PathVisio and Inkscape. Other photo editing and combination was done using Microsoft PowerPoint or Excel. Graphical representations were created in GraphPad Prism 5.

Design of guide RNA

Three exon regions for LDHA were chosen to be targeted. Long exons close to an ATG sequence were chosen. Feng Zhang's groups work was used to identify sequences, accessed at <http://crispr.mit.edu/>. For each exon region, both a forward and reverse primer were created.

Cloning of guide RNA in pCRISPRv2 Vector

The backbone was created using 4 µg -pCRISPRv2, 4 µL of 10x NEB 3.1, 2 µL BsmIB and H₂O to fill a final volume of 40 µL. This was left to incubate at 37°C for 4 hours.

After incubation, 1 µL CIP was added and this mixture was then incubated for 1 hour at 37°C. To purify the fragment, a Qiaquick Kit was used. To phosphorylate and anneal the oligomers, each oligomer was prepared by combining 180 µL H₂O with 10 µL of 100 µM oligomer 1 and 10 µL of 100 µM oligomer 2. Then, 1 µL of the oligomer preparation was added to 20 µL of H₂O and after this, 2 µL of 10x T4 ligase buffer containing ATP was added along with 1 µL of T4 PNK. Next, 80 µL of 1x T4 ligase buffer was added to each tube. The mixtures were then run in a thermocycler according to the following presets: 37°C for 45 minutes, then 95°C for 5 minutes and slowly dropped in temperature to

37°C. Ligation was achieved by combining the following mixture: 3 µL H₂O, 5 µL of 2x quick ligase buffer, 1 µL of pCRISPR v2 (about 30 ng), 1 µL of the diluted oligomer, and 1 µL of T4 ligase. This was then incubated for 30 minutes at room temperature. It is important to add the diluted oligomer last to the mixture. Transformation of the ligated oligomer was completed by the following process. First, by adding 10 µL of the ligation product to 100 µL of competent cells and placed on ice for 20 minutes. Second by placing the mixture in a 42°C water bath for 2 minutes, then back on ice for 2 minutes, then adding 600 µL of LB medium and incubating for 30 minutes at 37°C. After this incubation, half of the volume was plated in drops and then spread using a bent glass Pasteur pipette.

Screening of Positive Clones of gRNA

Preparation of the template was completed by addition of 22.5 µL water to a PCR tube for each clone. 5 clones of each ligation were picked. Clones were picked using a 20 µL tip and resuspended in the water in each PCR tube. Next, 100 µL LB media with ampicillin was added to a sterile 96 well plate for each of the picked clones. 10 µL of the E. coli suspension was added and incubated at 37°C to save as a “back-up”. For the PCR, the E. coli samples were boiled for 10 minutes at 95°C. While this was boiling, the following mixture was created for each template: 2.5 µL 10x B, 0.6 µL 10 mM dNTPS, 0.6 µL CRISPR forward and reverse, 0.3 µL Taq polymerase, 8.5 µL H₂O. After boiling, 12.5 µL of each boiled template was added to a PCR tube containing this mixture. For the PCR cycle, it was run at 95°C for 3 minutes, then 40 cycles of 95°C for 30 seconds, 50°C

for 30 seconds, 72°C for 30 seconds. Lastly the samples were held at 72°C for 5 minutes. The PCR products were run on a 1.5% gel to assess the efficiency. Two of the best products for each template were selected and inoculated in 5 mL of LB-Ampicillin for use in the Qiagen miniprep kit. The prepared samples were then sent for sequencing.

Preparation of Plasmids for LDHA expression

First, the CDC region of LDHA was analyzed and restriction enzymes were chosen. EcoRI and NotI restriction enzymes were chosen (New England BioLabs). The sequences of the Forward EcoRI and Reverse NotI are as follows:

| | |
|---------|-------------------------------------|
| EcoRI F | GGAATTCATGGCAACTCTAAAGGATC |
| NotI R | TTAAAATTGCAGCTCCTTTGCGGCCGCTAAACTAT |

Table 1: List of Primers used for the generation of Plasmids used for transfection of LDHA. EcoRI and NotI were chosen due to other possible enzymes displaying cutting sites that would inactivate the transfected plasmid.

After receipt of the primers, 100 µL of RNase Free water was added to create a working primer. The primers were then used in Reverse Transcription PCR to generate a PCR product to produce useable LDHA overexpression plasmids. cDNA generated from MCF-7 RNA was used in the Reverse Transcription PCR. 5 Plasmids were chosen to create 5 separate backbones, pCDH Puromycin, pCDH Flag Puromycin, pCDH COP GFP, pCDH Neomycin, and pCDH RFP Neomycin. From these, pCDH Puromycin, pCDH Flag Puromycin, and pCDH COP GFP were chosen to continue the experiments. The plasmids were first grown in a 3 mL volume of LBA⁺ medium and placed in a shaking incubator at 200 RPM at 37°C for 6 hours. After 6 hours, these cultures were

transferred to 100 mL total volume and placed back in the shaking incubator overnight at the same conditions. The plasmids were extracted the next morning using a Qiagen Maxi Kit. Following extraction, the plasmids were then purified on an 8% Agarose gel and subsequently extracted using a QIAquick Gel Extraction Kit (Qiagen). Following purification, the plasmids were ligated using the following procedure. To a 1.5 mL Eppendorf tube, 5 μ L of 2x quick ligase buffer, 1 μ L of plasmid backbone (pCDH Puro, pCDH Flag Puro, or pCDH COP GFP), 1 μ L of hLDHA PCR product, and 1 μ L of T4 ligase were added and incubated at RT for 30 minutes. Following ligation bacterial transformation was completed to obtain positive clones according to the following procedure: 10 μ L of the ligation product was added to 100 μ L of competent cells and incubated on ice for 20 minutes. After this incubation, the mixture was quickly transferred into a 42°C water bath to achieve heat shock for 2 minutes, then placed back on ice for 2 minutes. 600 μ L of LB medium was added to the mixture and incubated for 30 minutes at 37°C. After this incubation, the mixture was spun down and carefully decanted and the bacterial pellet was resuspended in 100 μ L of LB medium and plated onto an LBA⁺ agar plate. This plate was then incubated overnight at 37°C and clone growth was assessed 24 hours later and 5 large clones were picked. These clones were then expanded into 3 mL of LBA⁺ medium and grown overnight. The following morning the plasmids were extracted using a Qiagen Miniprep kit. The extracted plasmids were then analyzed for protein concentration. The two plasmids with the highest protein concentration were selected and sent for sequencing at the Harvard Medical School Biopolymers Facility.

Cell Culturing

MCF-7 Cells were cultured in DMEM, with 10% fetal bovine serum (FBS) as well as 1% penicillin and streptomycin. Cells were incubated in an atmosphere of 5% CO₂, and 95% O₂ at 37°C and humidified. DMEM, penicillin, and streptomycin were purchased from Fischer Scientific while the FBS was purchased from Atlanta Biologics. Cell lines were subcultured every 3 days.

Mouse SCLC cell lines were cultured in RPMI, with 10% fetal bovine serum (FBS) as well as 1% penicillin and streptomycin. Cells were incubated in an atmosphere of 5% CO₂, and 95% O₂ at 37°C and humidified. RPMI, penicillin, and streptomycin were purchased from Fischer Scientific while the FBS was purchased from Atlanta Biologics. Cell lines were subcultured every 3 days.

Western Blotting

Samples were prepared in equal concentrations to be run on an 8% Tris-Glycine gel. All samples were run for 15 minutes at 80 A, then 15 minute intervals of 150 A until ready to transfer and a last 20-minute interval of 50 A. Transferring was done onto a nitrocellulose membrane run at 400 mA for 1.5 hours at 4°C. After transferring, the membrane was blocked for 1 hour at RT using 5% milk in TBST. The primary antibody was incubated overnight at 4°C on a shaker. Following the incubation, three washes of 5 minutes with TBST were completed before the HRP Conjugated secondary antibody was incubated for 1 hour at RT. The membrane was again washed three times for 5 minutes each with TBST. The membrane was developed using Hyglo® Quick Spray and a dark room.

Protein Extraction and Concentration Detection

To extract protein from cells, the cells were aspirated and washed with PBS. Then a lysis buffer of 2% SDS was added to the cells. This mixture was then boiled for 20 minutes at 100°C. Protein concentration was detected using the Pierce™ BCA Protein Assay Kit.

RNA Extraction

Cells were aspirated and 800 µL of Trizol was added directly to the cells and incubated for 1 minute at RT. This mixture was then mixed in a pipette and transferred to a microcentrifuge tube and frozen. At a later time the RNA samples were thawed and vortexed. 200 µL of chloroform was added to each sample and vigorously mixed.

Samples were then centrifuged for 5 minutes at 12,000 g at 4°C. Aqueous phase was transferred to a fresh microcentrifuge tube and 500 µL of isopropanol was added.

Mixture was then incubated at RT for 10 minutes. Next the mixture was centrifuged for 10 minutes at 12,000 g at 4°C. Pellet was then washed with 800 µL of 70% RNase free Ethanol. Sample was then spun down and supernatant was removed. Pellet was dried at RT and then dissolved in RNase free water between 15 and 50 µL depending on pellet size to maintain similar concentrations. Concentration was measured using a NanoDrop spectrophotometer (Thermo Scientific).

Virus Transfection and Infection

Desired plasmids were transfected into Human Embryonic Kidney (HEK) 293T cells using Lipofectamine 2000 to create the required lentivirus. The medium was changed after 6 hours. 48 hours after initial transfection the lentivirus was harvested and the new cells were infected. 48 hours post infection the cells were selected using 2 µg/mL

puromycin. Cells were grown to full density and subcultured once before experiments were completed.

Lactate Studies

Cells were cultured according to previously listed methods and then plated on a 12 well plate with a glass sheet on the bottom in two cell numbers. Cells were counted with a hemocytometer and light microscope. Two time periods of lactate incubation were used, 24 hours and 48 hours.

Immunofluorescence Staining

Cells were seeded at either twenty-four or forty-eight hours prior to fixation. Fixation was done with a 4% solution of paraformaldehyde in phosphate buffered saline. Cells were then permeabilized and blocked in a solution of 0.5% Triton X-100 and 3% BSA in phosphate buffered saline at pH 7.5 for 30 minutes. Next, the cells were incubated with the primary antibody for 1 hour at room temperature. All antibodies were diluted in a solution of 1% BSA in phosphate buffered saline. Cells were then rinsed and washed with 0.1% phosphate buffered saline Triton X-100 (PBST). Next the cells were incubated with the secondary antibody for 1 hour at room temperature in complete darkness. Cells were then rinsed with PBST and mounted with Fluoromount-G medium and visualized via microscope.

Soft Agar Assay

For the soft agar assay, two layers of agarose were prepared in a 6 well plate. The bottom layer consisted of 1% agarose, which was diluted down from a 3% agarose stock with the medium of use for the cell line. This layer was incubated at 4°C to allow solidification.

The top layer was created by combining 3% agarose with 10% fetal bovine serum fortified medium, and 100% fetal bovine serum. This mixture initially created a 0.8% agarose mixture and was diluted with the correct number of cells in a 1:1 ratio to create a final concentration of 0.4% agarose. After plating the cells, the 6 well plate was placed into the 4°C fridge to solidify for 30 minutes before it was moved to the 37°C incubator with 5% CO₂. 500 µL of complete media was added every four days to the plated cells. After visual growth was visualized, the cells were stained with 1 mL p-iodonitrotetrazolium violet at 37°C overnight. Next, the plates were scanned and the stained colonies were counted.

RESULTS

Validation of pCDH Plasmids

Table 2: Concentration of pCDH Plasmids before ligation. Concentrations of pCDH Plasmids after initial growth, before ligation of LDHA PCR product with plasmid. High concentrations of plasmid were extracted with MaxiKit from Qiagen to have enough plasmid for other experiments and have sufficient stock.

| pCDH Plasmid | Concentration (ng/ μ L) |
|-------------------|-----------------------------|
| pCDH Neomycin | 1202.1 |
| pCDH Puromycin | 1126.9 |
| pCDH RFP Neomycin | 1420.7 |

Validation of hLDA sgRNA in MCF-7 cells

To ensure that the sgRNA for hLDHA was correct and accurate, the knock-out of LDHA was first assessed in MCF-7 cells. Protein concentration and subsequent western blot were completed to analyze knock-out efficiency.

Figure 3: Protein detection of hLDHA sgRNA in MCF-7 cells. Standard Curve for protein detection of hLDHA sgRNA in MCF-7 cells. Standards used were 0, 2, 4, 6, 8, 12, 16, and 20 μ g/mL of BSA.

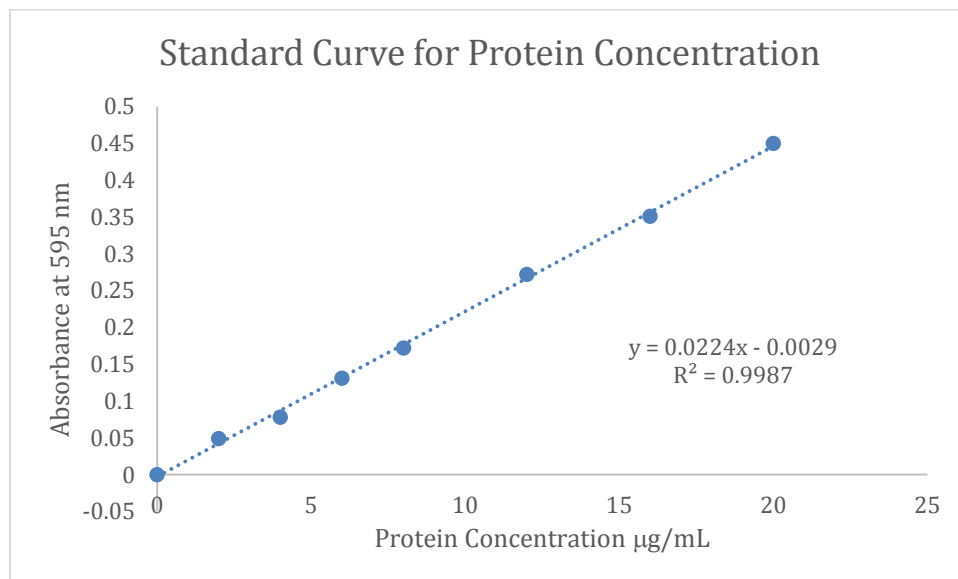
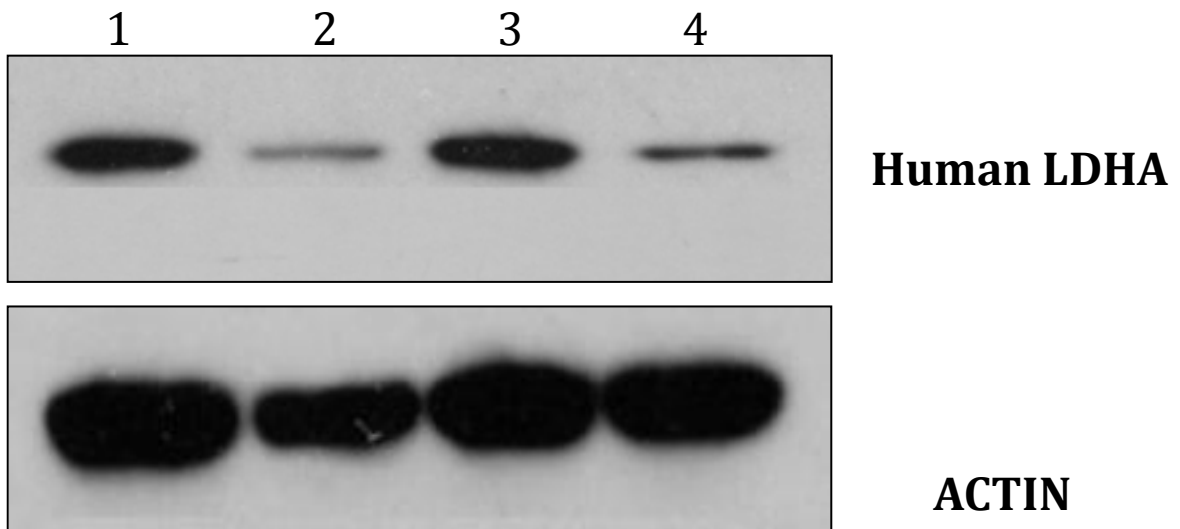


Table 3: Protein Concentration of MCF-7 hLDHA sgRNA Cells. Protein concentration of collected cells after 7 days, with 1 subculturing done in a 1:4 ratio. CRISPR V2 serves as the control cell line, and based on the protein concentration of hLDHA sgRNA 1 and 3 show that there is decreased growth of cell lines with hLDHA knocked out.

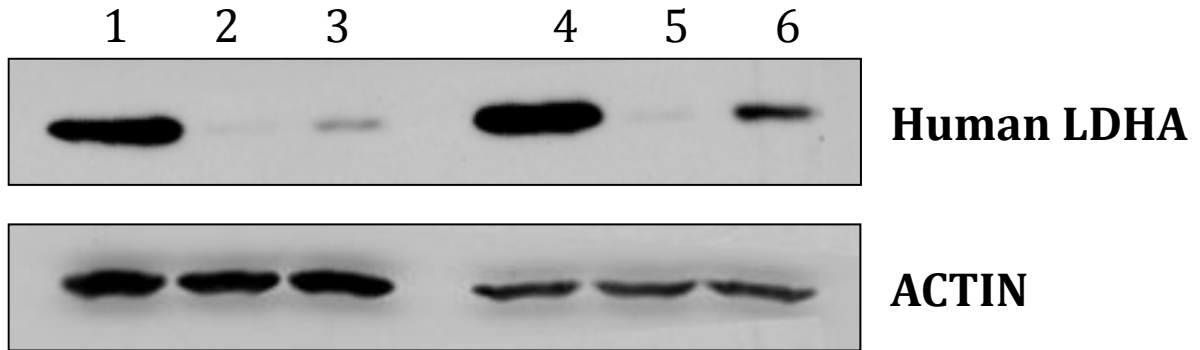
| Cell Modification | Protein Concentration ($\mu\text{g}/\text{mL}$) |
|---------------------|---|
| MCF-7 CRISPR V2 | 13.23 |
| MCF-7 hLDHA sgRNA-1 | 9.77 |
| MCF-7 hLDHA sgRNA-2 | 13.61 |
| MCF-7 hLDHA sgRNA-3 | 10.82 |

Figure 4: Western Blot of 2-day Puromycin Selection of MCF-7 Cells. A represents the Actin internal control while B 1-4 is MCF-7 cells with the following mutations: 1: CRISPER V2-puromycin, 2: hLDHA sgRNA 1-puromycin, 3: hLDHA sgRNA 2-puromycin, hLDHA sgRNA 3-puromycin.



Validation of hLDA sgRNA in A549 and MCF-7 cells

Figure 5: Western Blot of hLDHA-KO in MCF-7 and A549 Cells. A: Actin internal control, B: hLDHA. 1: MCF-7 CRISPR V2, 2: MCF-7 hLDHA sgRNA 1, 3: MCF-7 hLDHA sgRNA 2, 4: A549 CRISPR V2, 5: A549 hLDHA sgRNA 1, 6: A549 hLDHA sgRNA. Western blot shows confirmation of hLDHA knock-out efficiency in MCF-7 and A549 constructed cell lines after 1 week puromycin selection



LDHA Staining in A549 Lung Carcinoma Cells

Figure 6: IF Staining of A549 WT Cells in Full Medium. LDHA (green) staining in A549 wild type cells fixed after 24 hours of growth in full media. DAPI (blue) staining shows the nucleus of the cell. A: LDHA staining only, zoomed out view, B: DAPI staining only, zoomed out view, C: Merged LDHA and DAPI staining, zoomed out view, D: LDHA staining only, zoomed in view, E: DAPI staining only, zoomed in view, E: Merged LDHA and DAPI staining, zoomed in view. Objective magnification is 60X, with a total magnification of 600X.

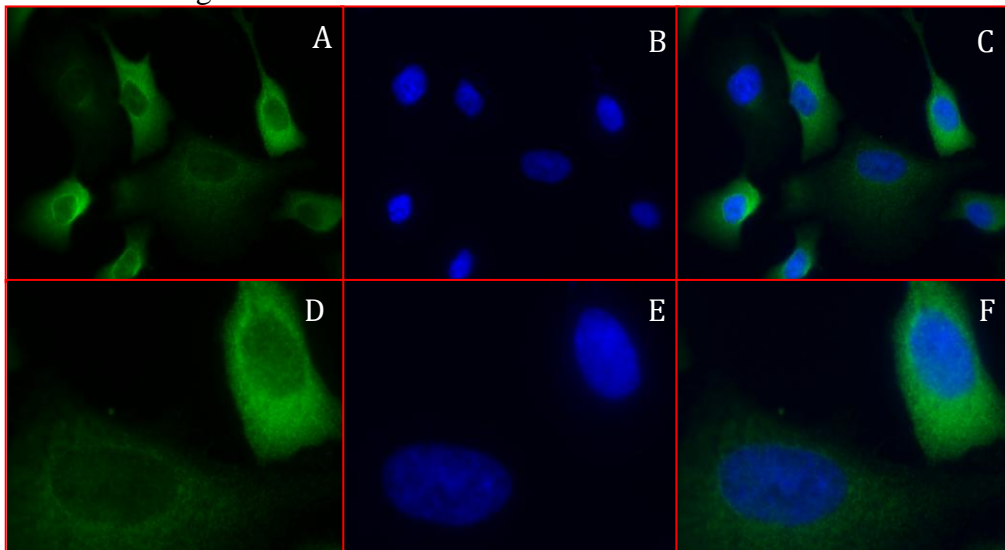


Figure 7: IF Staining of A549 WT Cells with Lactate Treatment. LDHA (green) staining in A549 wild type cells treated with Lactate (10 mM) for 24 hours and fixed. DAPI (blue) staining shows the nucleus of the cell. A: LDHA staining only, zoomed out view, B: DAPI staining only, zoomed out view, C: Merged LDHA and DAPI staining, zoomed out view, D: LDHA staining only, zoomed in view, E: DAPI staining only, zoomed in view, E: Merged LDHA and DAPI staining, zoomed in view Objective magnification is 60X, with a total magnification of 600X.

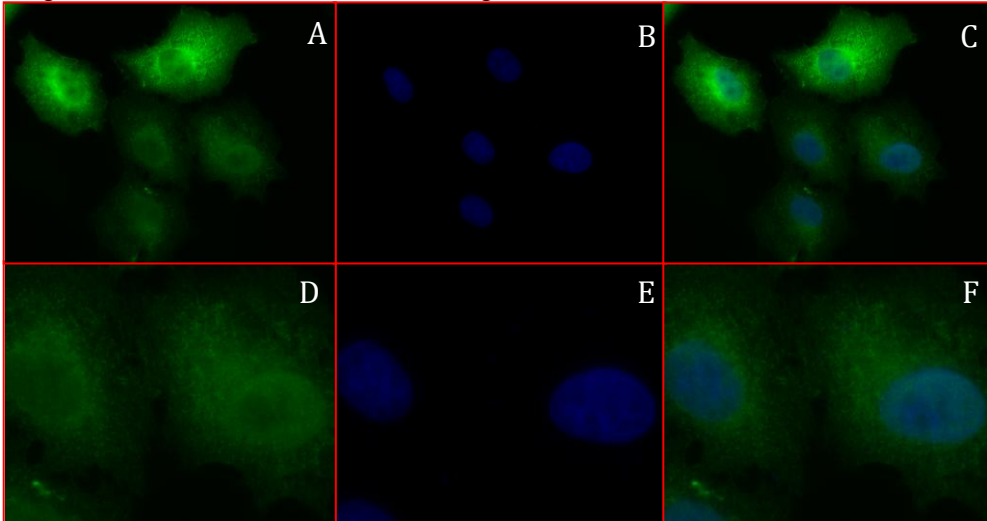


Figure 8: IF Staining of A549 CRISPR V2 Cells in Full Medium. LDHA (green) staining in A549 CRISPR V2 cells treated with full media for 24 hours and fixed. DAPI (blue) staining shows the nucleus of the cell. A: LDHA staining only, zoomed out view, B: DAPI staining only, zoomed out view, C: Merged LDHA and DAPI staining, zoomed out view, D: LDHA staining only, zoomed in view, E: DAPI staining only, zoomed in view, E: Merged LDHA and DAPI staining, zoomed in view. Objective magnification is 60X, with a total magnification of 600X.

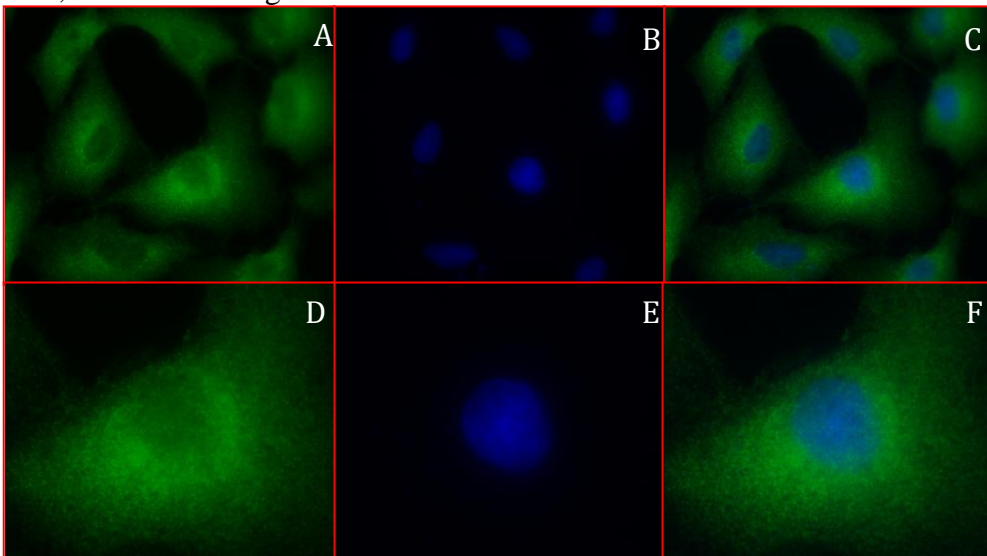


Figure 9: IF Staining of A549 CRISPR V2 Cells with Lactate Treatment. LDHA (green) staining in A549 CRISPR V2 cells treated with Lactate (10 mM) for 24 hours and fixed. DAPI (blue) staining shows the nucleus of the cell. A: LDHA staining only, zoomed out view, B: DAPI staining only, zoomed out view, C: Merged LDHA and DAPI staining, zoomed out view, D: LDHA staining only, zoomed in view, E: DAPI staining only, zoomed in view, E: Merged LDHA and DAPI staining, zoomed in view. Objective magnification is 60X, with a total magnification of 600X.

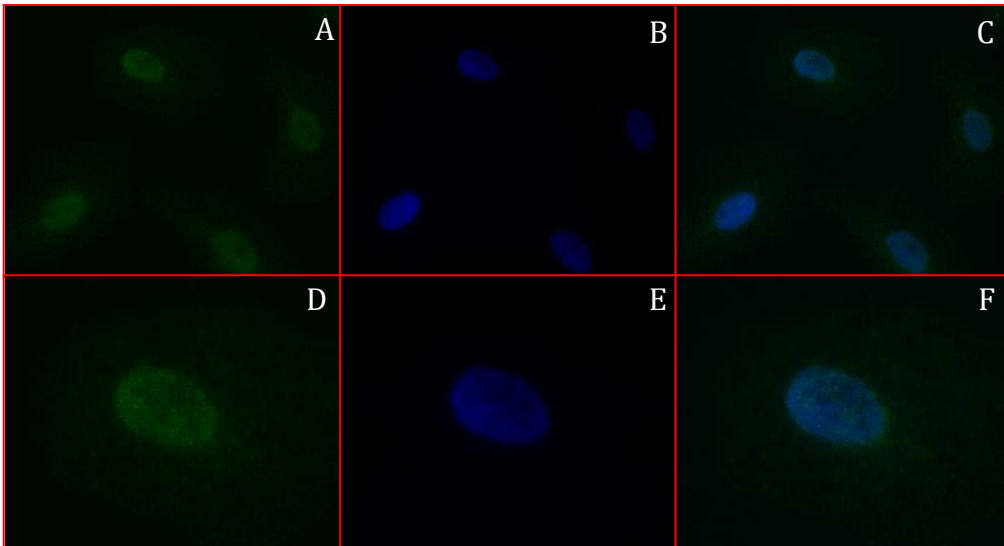
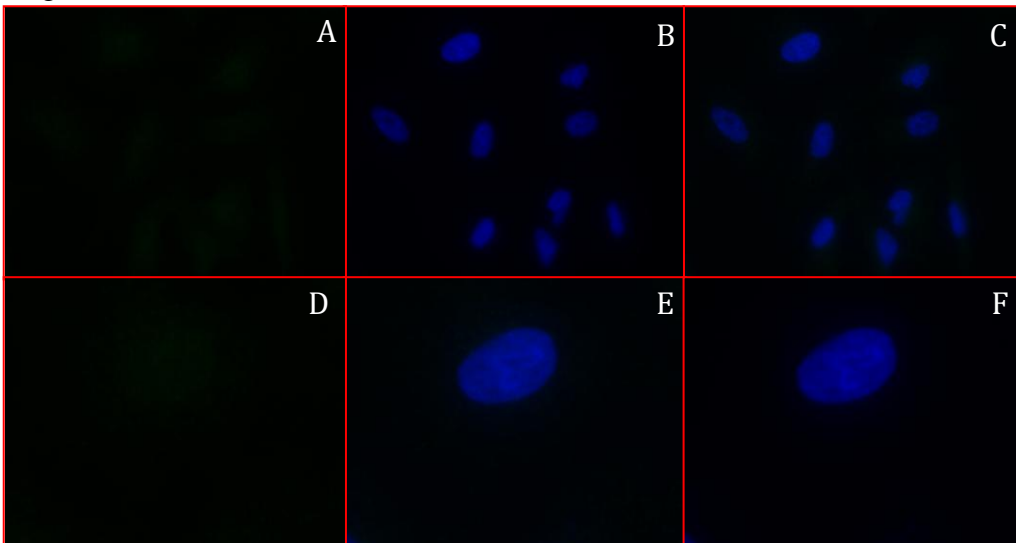


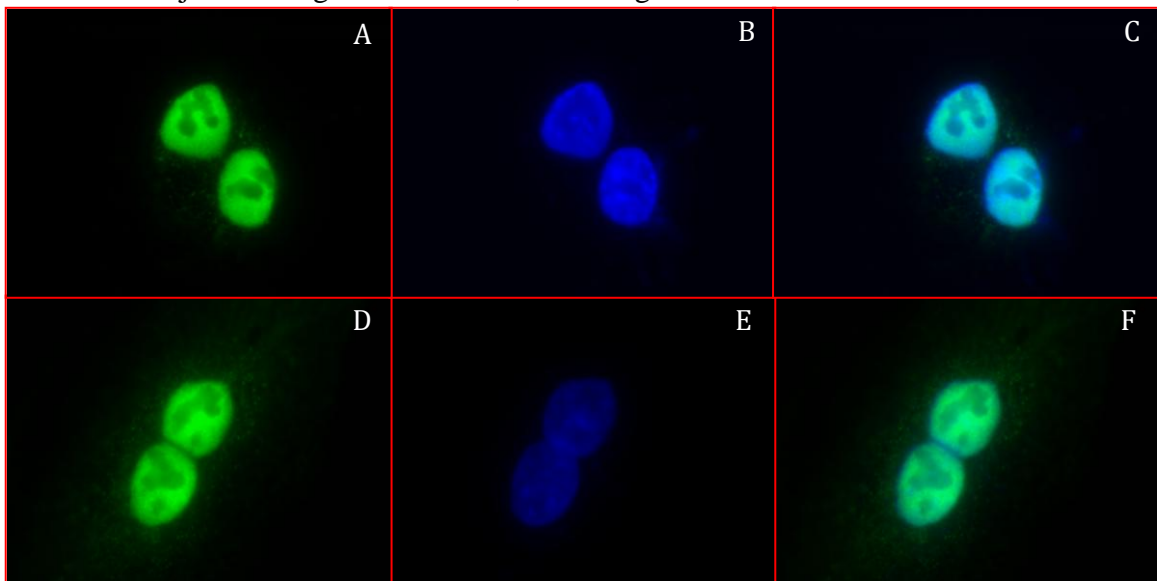
Figure 10: IF Staining of A549 hLDHA sg1 in Full Medium. LDHA (green) staining in A549 hLDHA sgRNA in full media. A: LDHA staining only, zoomed out view, B: DAPI staining, zoomed out, C: Merged LDHA and DAPI staining, zoomed out view, D: LDHA staining only, zoomed in view, E: DAPI staining only, zoomed in view, E: Merged LDHA and DAPI staining, zoomed in view. Objective magnification 60X, total magnification of 600X.



Immunofluorescence was performed on A549 hLDHA sgRNA 1 cells to confirm the population of cells where LDHA was knocked out. The DAPI serves as the denominator. The lack of hLDHA staining clearly shows that the sgRNA 1 was successfully integrated into the cell line.

Translocation of LDHA into the nucleus

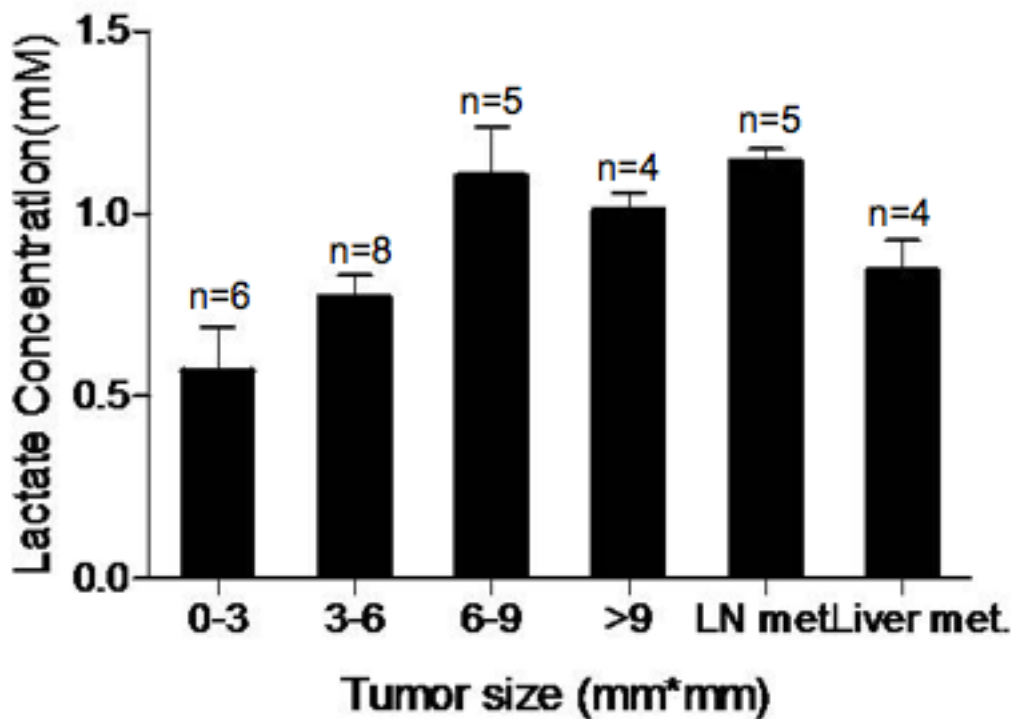
Figure 11: Translocation of LDHA into the Nucleus. LDHA (Green), and DAPI (Blue) staining in A549 Wild type cells (A, B, C) and A549 CRISPR V2 cells (D, E, F). These translocation pictures were found in the cells treated with full media and no lactate treatment. Objective magnification 60X, total magnification of 600X.



The translocation of LDHA into the nucleus was found to occur in both the A549 wild type cells as well as the A549 CRISPR V2 cells. These translocations occurred in both the no lactate treatment groups as well as the lactate treatment groups, with the lactate treatment having little to no effect on the translocation amount.

Concentration of lactate in different tumor samples

Figure 12: Concentration of Lactate in Different Sized Tumors. Concentration of lactate found in tumors from size 0 mm to greater than 9 mm, as well as different metastases of the tumors. As the tumor size increased, there was a higher concentration of lactate. Additionally, in the tumors sampled from a secondary site, there was a higher concentration of lactate, independent of size.



The general trend found in the presented data shows that as the tumor increased in size, there was more extracellular lactate present in the sample. Additionally, samples taken from a secondary site tended to have an increased concentration of lactate.

SCLC in 716T2S cells derived from mouse model

Figure 13: Expression of LDHA in 716T2S Cell Line. Western Blot of Four Mouse SCLC cell lines, 1 and 2 are cell lines with high LDHA expression and 3 and 4 are cell lines with low LDHA expression. GAPDH and ACTIN served as internal controls for the expression of LDHA.

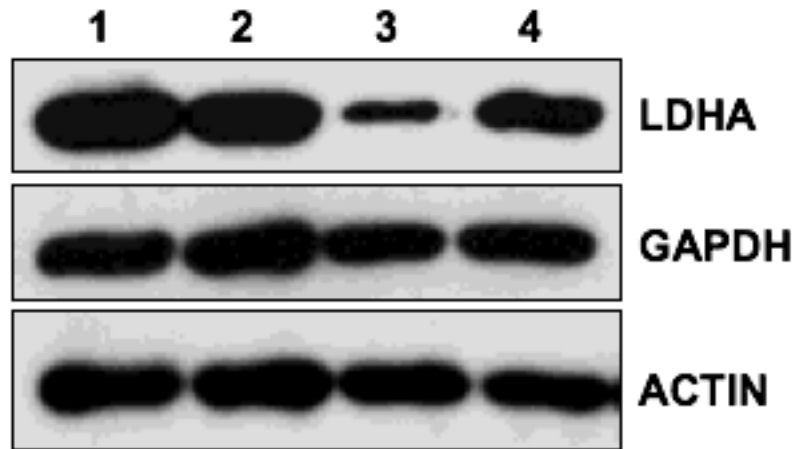


Figure 14: Lactate Concentration in Mouse SCLC Cells. Detection of intracellular Lactate concentration in the high LDHA and low LDHA expressing cell lines. Expression was normalized to a wild type control such that relative expression could be graphed.

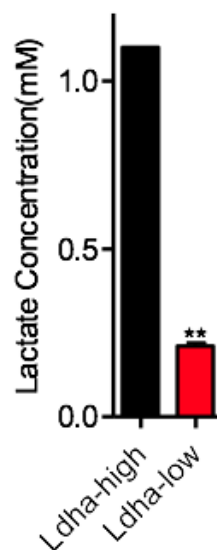


Figure 15: Western Blot of LDHA-KO in Mouse SCLC Cells. Western blot of 716T2S cell lines with the two separate LDHA sgRNAs to show the knockout of LDHA. Actin served as the internal control and the CRISPR V2 cell line served as the cell control.

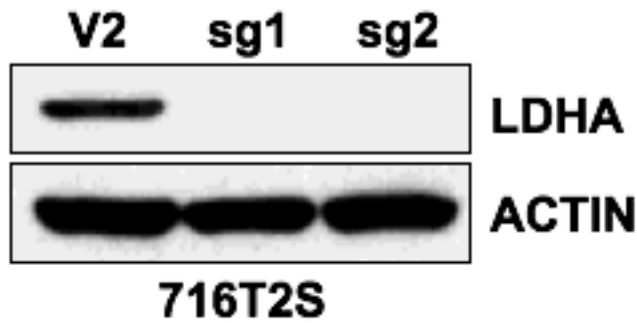


Figure 16: Lactate Concentration in 716T2S-LDHA-KO Cells. Knock out of LDHA in a high LDHA expressing cell line, 716T2N. CRISPR V2 was used as the control for the transfection of the LDHA sgRNA1 and 2. *** means $p < .05$. Two separate LDHA sgRNAs were designed and transfected into the cells.

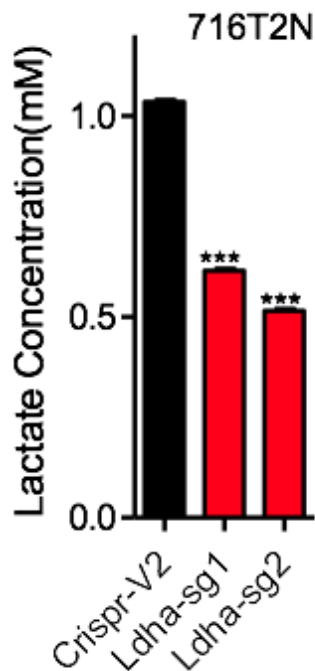


Figure 17: Colony Formation of 716T2S-LDHA-KO cells. Soft Agar Assay of 716T2S cell lines. Left: 716T2S CRISPR V2 control cell line, Middle: 716T2S LDHA-sgRNA 1 cell line, Right: 716T2S LDHA-sgRNA 2 cell line.

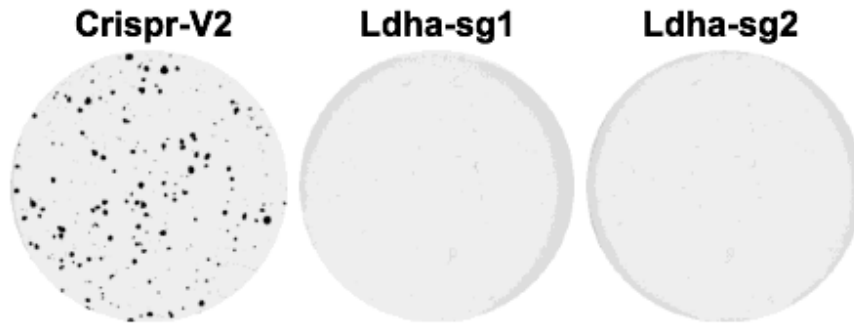


Figure 18: Colony Counting of 716T2S-LDHA-KO Cells. Count of the colony growth from the soft agar assay of the 716T2S CRISPR V2, 716T2S LDHA-sgRNA 1, 716T2S LDHA-sgRNA 2 cells. *** means $p < .05$.

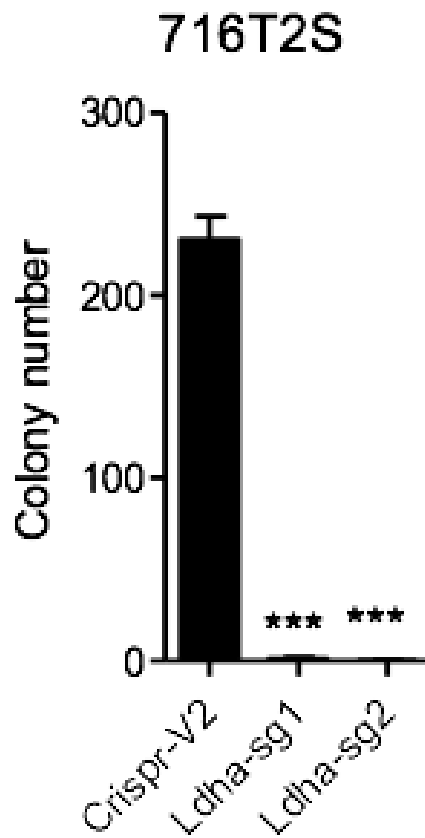
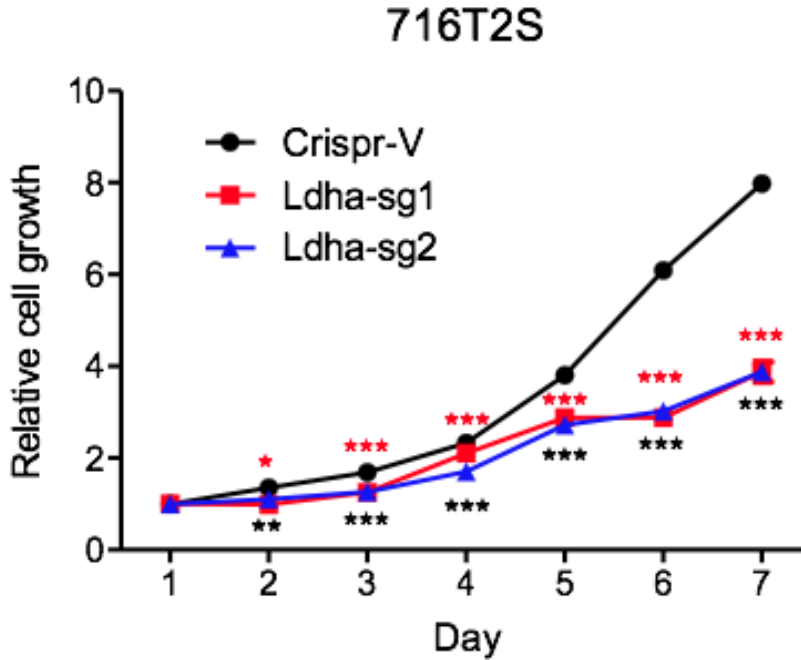


Figure 19: Cellular Growth of 716T2S-LDHA-KO Cells. Graphical representation of the growth inhibition caused by the absence of LDHA in the 716T2S cell lines. Cells were analyzed in twenty-four hour increments for seven days to analyze growth.



SCLC in 728N cells derived from mouse model

Figure 20: Western Blot of 728N-LDHA-KO Cells. Western blot showing the efficiency of knockout of LDHA in the mouse model derived 728N cell line. Left: 728N CRISPR V2 cells, Middle: 728N LDHA sg1, Right 728N LDHA sg2. Actin served as the internal control. Knockout was successful in generating two stable clone cell lines for experiments.

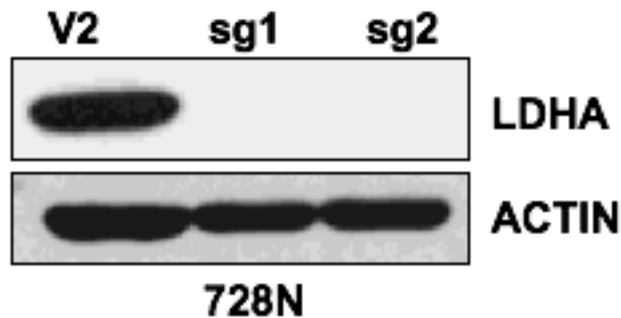


Figure 21: Colony Formation of 728N-LDHA-KO Cells. Soft Agar Assay of 728N mouse model derived cell line. Left: 728N CRISPR V2, Middle: 728N LDHA sg1, Right: 728N LDHA sg2. Colony growth was greatly inhibited by the lack of LDHA in the cell.

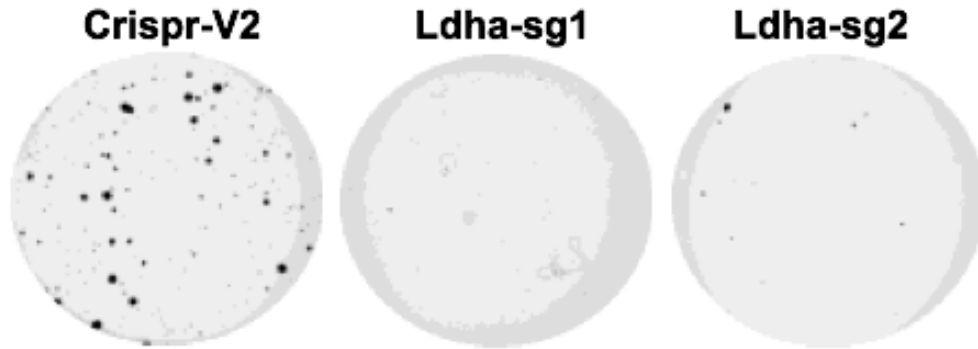


Figure 22: Colony Counting of 728N-LDHA-KO Cells. Graphical representation of the Colony number found in the Soft Agar Assay of the mouse model derived 728N cells. Left: 728N CRISPR V2, Middle: 728N LDHA sg1, Right: 728N LDHA sg2. *** means $p < .05$

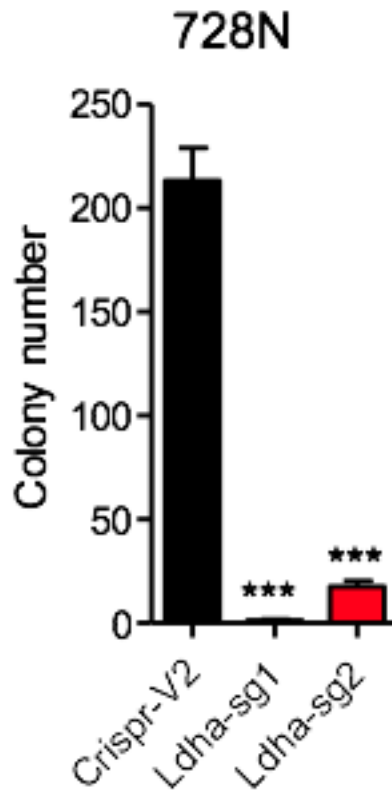
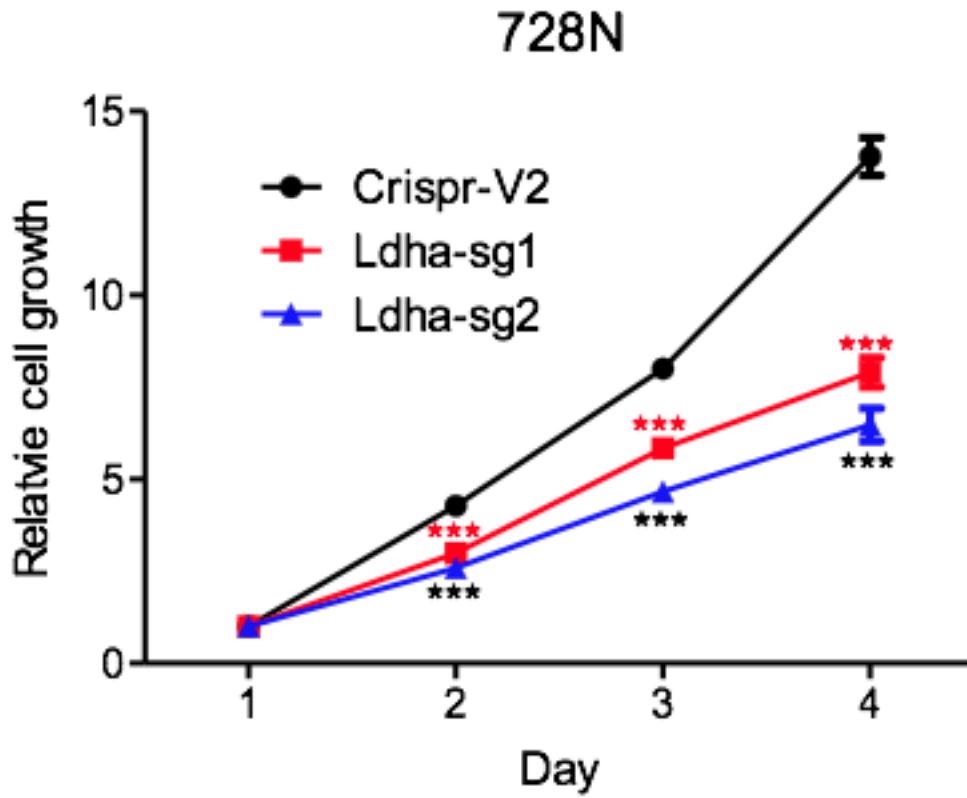


Figure 23: Cellular Growth of 728N-LDHA-KO Cells. Results of the MTT assay. Black line: Growth of 728N CRISPR V2 cells, Red line: Growth of the 728N LDHA sg1 cells, Blue line: Growth of 728N LDHA sg2 cells. Growth of the LDHA knockout cell lines was impacted greatly by the lack of LDHA in the cell. *** means $p < .05$.



DISCUSSION

The treatment of SCLC continues to provide a difficult challenge, as no targeted therapy has been developed even as combinations of immunotherapy and chemotherapy are being implemented with various degrees of success in other cancer types. Part of the lack of treatment options may lie in the difficulty of obtaining primary samples of SCLC tumors. However, until recently, there has also been a distinct lack of research into SCLC. As the technology used in research continues to advance, there has been progress into the research of SCLC. This study sought to elucidate what role, if any, that LDHA had in the progression of SCLC. If there is a way to successfully decrease the vitality of a cancer cell by targeting LDHA, that provides the basis for using either an inhibitor of LDHA or eventually the knock-out of LDHA using gene editing technology. By using the inhibition or removal of LDHA in combination with other targeted therapies, this might improve the success rates of cancer therapy. LDHA knock-out studies were done in mouse SCLC cell lines, which are in some ways similar, but in others are different from human SCLC cell lines. The difficulty in using human SCLC cell lines is that currently there is a lack of samples as it is a highly metastatic cancer and that often times the complexity of the cell lines is rudimentary compared to the actual tumor cells. As mentioned earlier, SCLC is a highly heterogenic cancer type composed of both neuroendocrine and non-neuroendocrine cells. This ratio is subject to change based on the tumor's microenvironment and this increases the difficulty of culturing a completely faithful cancer cell line.

For the generation of sgRNA for LDHA the primers were first validated in MCF-7 and A549 cell lines. The two best sgRNAs were selected to continue experiments. The purpose of using MCF-7 and A549 cell lines to validate the primers was to have two different types of cancer cell lines to validate the knock-out of hLDHA. In the MCF-7 cell lines it was shown that there was a slight decrease in the amount of growth of the cell lines after hLDHA knock-out compared to wild type and CRISPR V2 controls. This indicated that there may be decreased viability of the cancer cell lines without LDHA present. Lactate studies were only performed on the A549 cell lines due to the focus of the study being lung cancer and not breast cancer.

The lactate studies were done at two different concentrations and two different time points to determine which would be the best. After examination of the immunofluorescence staining and pH of the medium, it was determined that there was no significant difference between the twenty-four hour lactate treatment and the forty-eight hour lactate treatment. The twenty-four hour lactate treatment was then repeated again. In both the A549 CRISPR V2 cells and the A549 wildtype cells, there was a slight decrease in the visible brightness of the LDHA staining in the lactate treated cells compared to control (Figures 6-10). This was expected as LDHA catalyzes the reversible reaction between pyruvate and lactate. It was expected that the increased lactate concentration would reduce the expression of LDHA as the cells attempted to maintain a stable microenvironment. The knock-out of LDHA in the A549 cells was very successful and was confirmed by both Western Blot and immunofluorescence. As there was very little

LDHA present in the A549 hLDHA sgRNA 1 cells, there was very little effect of the lactate treatment on the levels of LDHA present in the cells.

In the lactate studies, there was an unexpected result that was found, the translocation of LDHA into the nucleus, as visualized in the immunofluorescence staining (Figure 11). Interestingly, the translocation of lactate did not seem to be caused by the lactate, as it was present in both the control and lactate treated cells. The number of translocations that were in each immunofluorescence staining was very low, and the majority of the translocations were found around the outside of the cell plate. This suggested that perhaps the translocations were more likely to occur when there was a lower cell count that was seeded. This proved not to be the case as there was no significant difference in translocations between the cells seeded at 5000 cells per microliter and 2500 cells per microliter. The next question that we then sought to address was if the translocations occurred due to some technique in the staining process. The first variable that we changed was the shape of the plate that the cells were seeded on. The original plate shape was a circle. The circular plate was then completed in tandem with a square cell plate. There was not a significant variation in the number of translocations that appeared between the circular and square pieces of cover glass. However, the translocations did appear at a higher frequency along the outside of the cover glass, for both the square and the circular experiments.

From the studies in mouse SCLC cell lines, several observations were made. First, was the amount of lactate in different sized SCLC tumors (Figure 12). As the tumors became larger, the amount of lactate found in the tumor also increased. This result is not

completely unexpected due to what is known about hypoxia in tumors. As the tumor increases in size, the entire tumor is not perfused to the same degree, meaning that the portions without a reliable blood flow will be required to undergo anaerobic respiration more often. The interesting result is that of the increased concentration of lactate found in the metastatic samples of SCLC. This indicates that there is a potential role that LDHA might play in increasing the metastatic capability of tumors. Previous studies have suggested that increased LDHA increases the amount of necessary nutrients that can be taken up into the cell (Miller et al., 2012). With pharmacologic intervention against LDHA, it may be possible to slow the metastases of tumors. Second, there were tumor samples that had high expression of LDHA as well as samples with low expression of LDHA. Unsurprisingly, the samples with higher expression of LDHA also had higher levels of intercellular lactate (Figure 14). As there is more of the enzyme present, it is not difficult to understand why there is a higher amount of lactate produced by that tumor. It was also found that by knocking out LDHA in both of these sample types, that the concentration of lactate decreased when compared to control (Figure 16).

Following the Soft Agar Assay, it was clear to see how the knock-out of LDHA inhibited the colony growth of the mouse SCLC cell lines. Compared to control there was significantly decreased growth of the LDHA KO cell lines. This experiment showed the potential therapeutic avenue that arises through treatment of SCLC by inhibiting LDHA's activity in vitro. This opens up treatment of SCLC cell lines with specific LDHA inhibitors that could be used in a combination therapy along with other drugs target to SCLC. Further studies need to be continued to provide more insight into treatment of

SCLC, however the validation of LDHA as a potential target will help. There are inhibitors of LDHA that could be used *in vitro*, which is the next step of this research. By inhibiting LDHA pharmacologically it would be interesting to confirm if the colony growth and cellular growth of tumors is affected in the same manner. Pharmacological inhibition would be more suitable for clinical treatment than using genetic knock-outs, due to the limited effectiveness of the CRISPR-cas9 system in targeting specific sites. As more research is completed when looking into LDHA and its link to cancer, it is possible that there are novel drug designs that will be able to effectively and selectively target LDHA. As the development of drugs and research progresses, hopefully a manageable treatment for SCLC will emerge, and provide relief to a once recalcitrant disease.

REFERENCES

- An, J., Zhang, Y., He, J., Zang, Z., Zhou, Z., Pei, X., ... Li, S. (2017). Lactate dehydrogenase A promotes the invasion and proliferation of pituitary adenoma. *Scientific Reports*, 7(1), 4734. <https://doi.org/10.1038/s41598-017-04366-5>
- Bohn, T., Rapp, S., Luther, N., Klein, M., Bruehl, T.-J., Kojima, N., ... Bopp, T. (2018). Tumor immunoevasion via acidosis-dependent induction of regulatory tumor-associated macrophages. *Nature Immunology*, 19(12), 1319. <https://doi.org/10.1038/s41590-018-0226-8>
- Chen, C., Zhu, Y.-H., & Huang, J.-A. (2018). Clinical evaluation of potential usefulness of serum lactate dehydrogenase level in follow-up of small cell lung cancer. *Journal of Cancer Research and Therapeutics*, 14(Supplement), S336–S340. <https://doi.org/10.4103/0973-1482.168994>
- Chen, Y., Yang, X., Xu, Y., Cao, J., & Chen, L. (2017). Genomic analysis of drug resistant small cell lung cancer cell lines by combining mRNA and miRNA expression profiling. *Oncology Letters*, 13(6), 4077–4084. <https://doi.org/10.3892/ol.2017.5967>
- Deng, T., Zhang, J., Meng, Y., Zhou, Y., & Li, W. (2018). Higher pretreatment lactate dehydrogenase concentration predicts worse overall survival in patients with lung cancer. *Medicine*, 97(38). <https://doi.org/10.1097/MD.00000000000012524>
- Fadaka, A., Ajiboye, B., Ojo, O., Adewale, O., Olayide, I., & Emuowhochere, R. (2017). Biology of glucose metabolism in cancer cells. *Journal of Oncological Sciences*, 3(2), 45–51. <https://doi.org/10.1016/j.jons.2017.06.002>

- Gazdar, A. F., Bunn, P. A., & Minna, J. D. (2017). Small-cell lung cancer: what we know, what we need to know and the path forward. *Nature Reviews Cancer*, *17*(12), 725–737. <https://doi.org/10.1038/nrc.2017.87>
- Gray, L. R., Tompkins, S. C., & Taylor, E. B. (2014). Regulation of pyruvate metabolism and human disease. *Cellular and Molecular Life Sciences*, *71*(14), 2577–2604. <https://doi.org/10.1007/s00018-013-1539-2>
- Grosse, F., Nasheuer, H. P., Scholtissek, S., & Schomburg, U. (1986). Lactate dehydrogenase and glyceraldehyde-phosphate dehydrogenase are single-stranded DNA-binding proteins that affect the DNA-polymerase-alpha-primase complex. *European Journal of Biochemistry*, *160*(3), 459–467.
- Hanahan, D., & Weinberg, R. A. (2011). Hallmarks of Cancer: The Next Generation. *Cell*, *144*(5), 646–674. <https://doi.org/10.1016/j.cell.2011.02.013>
- Jansen, M. P. H. M., Foekens, J. A., van Staveren, I. L., Dirkzwager-Kiel, M. M., Ritstier, K., Look, M. P., ... Berns, E. M. J. J. (2005). Molecular Classification of Tamoxifen-Resistant Breast Carcinomas by Gene Expression Profiling. *Journal of Clinical Oncology*, *23*(4), 732–740. <https://doi.org/10.1200/JCO.2005.05.145>
- Jin, L., Chun, J., Pan, C., Alesi, G. N., Li, D., Magliocca, K. R., ... Kang, S. (2017). Phosphorylation-mediated activation of LDHA promotes cancer cell invasion and tumour metastasis. *Oncogene*, *36*(27), 3797–3806. <https://doi.org/10.1038/onc.2017.6>
- Kim, J., & Dang, C. V. (2005). Multifaceted roles of glycolytic enzymes. *Trends in Biochemical Sciences*, *30*(3), 142–150. <https://doi.org/10.1016/j.tibs.2005.01.005>

- Li, X.-M., Xiao, W.-H., & Zhao, H.-X. (2017). Discovery of potent human lactate dehydrogenase A (LDHA) inhibitors with antiproliferative activity against lung cancer cells: virtual screening and biological evaluation †The authors declare no competing interests. *MedChemComm*, 8(3), 599–605.
<https://doi.org/10.1039/c6md00670a>
- Liberti, M. V., & Locasale, J. W. (2016). The Warburg Effect: How Does it Benefit Cancer Cells? *Trends in Biochemical Sciences*, 41(3), 211–218.
<https://doi.org/10.1016/j.tibs.2015.12.001>
- Maiso, P., Huynh, D., Moschetta, M., Sacco, A., Aljawai, Y., Mishima, Y., ... Ghobrial, I. M. (2015). Metabolic signature identifies novel targets for drug resistance in multiple myeloma. *Cancer Research*, 75(10), 2071–2082.
<https://doi.org/10.1158/0008-5472.CAN-14-3400>
- Majmundar, A. J., Wong, W. J., & Simon, M. C. (2010). Hypoxia-Inducible Factors and the Response to Hypoxic Stress. *Molecular Cell*, 40(2), 294–309.
<https://doi.org/10.1016/j.molcel.2010.09.022>
- Markert, C. L. (1963). Lactate Dehydrogenase Isozymes: Dissociation and Recombination of Subunits. *Science (New York, N.Y.)*, 140(3573), 1329–1330.
<https://doi.org/10.1126/science.140.3573.1329>
- Masoud, G. N., & Li, W. (2015). HIF-1 α pathway: role, regulation and intervention for cancer therapy. *Acta Pharmaceutica Sinica. B*, 5(5), 378–389.
<https://doi.org/10.1016/j.apsb.2015.05.007>

- Miao, P., Sheng, S., Sun, X., Liu, J., & Huang, G. (2013). Lactate dehydrogenase a in cancer: A promising target for diagnosis and therapy. *IUBMB Life*, 65(11), 904–910. <https://doi.org/10.1002/iub.1216>
- Miller, D. M., Thomas, S. D., Islam, A., Muench, D., & Sedoris, K. (2012). c-Myc and Cancer Metabolism. *Clinical Cancer Research : An Official Journal of the American Association for Cancer Research*, 18(20), 5546–5553. <https://doi.org/10.1158/1078-0432.CCR-12-0977>
- Muz, B., de la Puente, P., Azab, F., & Azab, A. K. (2015). The role of hypoxia in cancer progression, angiogenesis, metastasis, and resistance to therapy. *Hypoxia*, 3, 83–92. <https://doi.org/10.2147/HP.S93413>
- Ooi, A. T., & Gomperts, B. N. (2015). Molecular Pathways: Targeting Cellular Energy Metabolism in Cancer via Inhibition of SLC2A1 and LDHA. *Clinical Cancer Research : An Official Journal of the American Association for Cancer Research*, 21(11), 2440–2444. <https://doi.org/10.1158/1078-0432.CCR-14-1209>
- Osthus, R. C., Shim, H., Kim, S., Li, Q., Reddy, R., Mukherjee, M., ... Dang, C. V. (2000). Deregulation of glucose transporter 1 and glycolytic gene expression by c-Myc. *The Journal of Biological Chemistry*, 275(29), 21797–21800. <https://doi.org/10.1074/jbc.C000023200>
- Parra-Bonilla, G., Alvarez, D. F., Al-Mehdi, A.-B., Alexeyev, M., & Stevens, T. (2010). Critical role for lactate dehydrogenase A in aerobic glycolysis that sustains pulmonary microvascular endothelial cell proliferation. *American Journal of*

Physiology - Lung Cellular and Molecular Physiology, 299(4), L513.

<https://doi.org/10.1152/ajplung.00274.2009>

Pavlova, N. N., & Thompson, C. B. (2016). THE EMERGING HALLMARKS OF CANCER METABOLISM. *Cell Metabolism*, 23(1), 27–47.

<https://doi.org/10.1016/j.cmet.2015.12.006>

Pilon-Thomas, S., Kodumudi, K. N., El-Kenawi, A. E., Russell, S., Weber, A. M., Luddy, K., ... Gillies, R. J. (2016). Neutralization of Tumor Acidity Improves Antitumor Responses to Immunotherapy. *Cancer Research*, 76(6), 1381–1390.

<https://doi.org/10.1158/0008-5472.CAN-15-1743>

Rhim, T., Lee, D. Y., & Lee, M. (2013). Hypoxia as a target for tissue specific gene therapy. *Journal of Controlled Release: Official Journal of the Controlled Release Society*, 172(2), 484–494. <https://doi.org/10.1016/j.jconrel.2013.05.021>

Rudin, C. M., Ismaila, N., Hann, C. L., Malhotra, N., Movsas, B., Norris, K., ... Giaccone, G. (2015). Treatment of Small-Cell Lung Cancer: American Society of Clinical Oncology Endorsement of the American College of Chest Physicians Guideline. *Journal of Clinical Oncology*, 33(34), 4106–4111.

<https://doi.org/10.1200/JCO.2015.63.7918>

Seki, S. M., & Gaultier, A. (2017). Exploring Non-Metabolic Functions of Glycolytic Enzymes in Immunity. *Frontiers in Immunology*, 8.

<https://doi.org/10.3389/fimmu.2017.01549>

Seth, P., Csizmadia, E., Hedblom, A., Vuerich, M., Xie, H., Li, M., ... Wegiel, B. (2017). Deletion of Lactate Dehydrogenase-A in Myeloid Cells Triggers Antitumor

- Immunity. *Cancer Research*, 77(13), 3632–3643. <https://doi.org/10.1158/0008-5472.CAN-16-2938>
- Seth, P., Grant, A., Tang, J., Vinogradov, E., Wang, X., Lenkinski, R., & Sukhatme, V. P. (2011). On-target inhibition of tumor fermentative glycolysis as visualized by hyperpolarized pyruvate. *Neoplasia (New York, N.Y.)*, 13(1), 60–71.
- Sharief, F. S., Wilson, S. H., & Li, S. S. (1986). Identification of the mouse low-salt-eluting single-stranded DNA-binding protein as a mammalian lactate dehydrogenase-A isoenzyme. *Biochemical Journal*, 233(3), 913–916.
- Shukla, V., Rao, M., Zhang, H., Beers, J., Wangsa, D., Wangsa, D., ... Schrump, D. S. (2017). ASXL3 is a Novel Pluripotency Factor in Human Respiratory Epithelial Cells and a Potential Therapeutic Target in Small Cell Lung Cancer. *Cancer Research*, 77(22), 6267–6281. <https://doi.org/10.1158/0008-5472.CAN-17-0570>
- Torre, L. A., Bray, F., Siegel, R. L., Ferlay, J., Lortet-Tieulent, J., & Jemal, A. (2015). Global cancer statistics, 2012. *CA: A Cancer Journal for Clinicians*, 65(2), 87–108. <https://doi.org/10.3322/caac.21262>
- Vander Heiden, M. G., Cantley, L. C., & Thompson, C. B. (2009). Understanding the Warburg effect: the metabolic requirements of cell proliferation. *Science (New York, N.Y.)*, 324(5930), 1029–1033. <https://doi.org/10.1126/science.1160809>
- Williams, K. R., Reddigari, S., & Patel, G. L. (1985). Identification of a nucleic acid helix-destabilizing protein from rat liver as lactate dehydrogenase-5. *Proceedings of the National Academy of Sciences of the United States of America*, 82(16), 5260–5264.

- Ždralović, M., Brand, A., Di Ianni, L., Dettmer, K., Reinders, J., Singer, K., ... Kreutz, M. (2018). Double genetic disruption of lactate dehydrogenases A and B is required to ablate the “Warburg effect” restricting tumor growth to oxidative metabolism. *The Journal of Biological Chemistry*, 293(41), 15947–15961. <https://doi.org/10.1074/jbc.RA118.004180>
- Zeller, K. I., Jegga, A. G., Aronow, B. J., O’Donnell, K. A., & Dang, C. V. (2003). An integrated database of genes responsive to the Myc oncogenic transcription factor: identification of direct genomic targets. *Genome Biology*, 4(10), R69.
- Zhao, Y. H., Zhou, M., Liu, H., Ding, Y., Khong, H. T., Yu, D., ... Tan, M. (2009). Upregulation of lactate dehydrogenase A by ErbB2 through heat shock factor 1 promotes breast cancer cell glycolysis and growth. *Oncogene*, 28(42), 3689–3701. <https://doi.org/10.1038/onc.2009.229>
- Zheng, L., Roeder, R. G., & Luo, Y. (2003). S Phase Activation of the Histone H2B Promoter by OCA-S, a Coactivator Complex that Contains GAPDH as a Key Component. *Cell*, 114(2), 255–266. [https://doi.org/10.1016/S0092-8674\(03\)00552-X](https://doi.org/10.1016/S0092-8674(03)00552-X)

VITA

